1st International Symposium on Laser Ultrasonics: Science, Technology and Applications
July 16-18 2008, Montreal, Canada

B-scan Simulations with Abaqus for Laser Ultrasonic Inspection of Structures

Michel ARRIGONI [1], Qiaosheng HU [2], Michel BOUSTIE [3], Laurent BERTHE [4], and Jean-Pierre MONCHALIN [5]

[1] Laboratoire Brestois de Mécanique et des Systèmes (Equipe d'Accueil 4325 - ENSIETA / Université de Brest / ENIB), 2 Rue François Verny, 29806 Brest Cedex 9 France; Phone: +33298348978, Fax : +33298348730; e-mail: michel.arrigoni@ensieta.fr
[2] 5-103 Jiading Campus, Tongji University, Shanghai, 201804, China; Phone: +8613917936477, Fax: +8602169589512, e-mail: huli2001_ren@163.com
[3] Laboratoire de Combustion et Détonique, CNRS UPR 9028, ENSMA, 1 avenue Clément Ader, 86960 Chasseneuil Futuroscope Cedex, France; Phone: +33 549498162, Fax:+ 33 549498176, email: boustie@lcd.ensma.fr
[4] Laboratoire d'Application des Lasers de Puissance, CNRS UPR 1578, GERAILP, 16 bis avenue du Prieur de la côte d'or, 94114 Arcueil Cedex, France; Phone: +33 142319981, Fax:+ 33 142319747, email: lberthe@gmail.com
[5] Institut des Matériaux Industriels, CNRC-NRC, Optical Diagnostics of Materials, 75 de Mortagne blvd., Boucherville (QC), J4B 6Y4, Canada; Phone: +1 450 641-5116, Fax: +1 450 641-5106; e-mail : Jean-Pierre.Monchalin@cnrc-nrc.gc.ca

Abstract
A recurrent challenge for inspection techniques in critical structural adhesive bonded parts is the detection of kissing bonds. An interesting alternative technique being developed is a laser based shock wave adhesion test, which manages to generate high tensile stresses in specific locations of the part that can delaminate weak bonds. In this paper, we analyze both theoretically an experimentally an alternative way of generating tensile stresses on materials with lasers. The experimental results, represented by B-scans on aluminium plates, clearly shows the configurations where tensile stresses are generated. Other than the information about the shock wave arrival at the free surface, the recorded signals allows determining stress history occurring in the target by an inverse method. Numerical simulation with the finite element analysis code ABAQUS CAE was found to reproduce experimental B-scans.
Keywords: Laser ultrasonics, B-scan, bond inspection, adhesion test, shock wave

1. Introduction

Laser ultrasonic inspection has had success in inspecting high critical components in aerospace industry [1,2]. However, some defects like kissing bonds are difficult to detect. Kissing bonds look as good bonds when tested with current non-destructive method but fails with much lower stresses. The lack of reliable non-destructive techniques that can detect kissing bonds has prevented a widespread adoption of adhesive bond for many critical applications. One emerging alternative to adhesive bonding inspection is the use of lasers to generate shock waves [3-6].

This paper presents experimental results of laser-induced shock waves generated by the laser and detected on the opposite surface of the plate. The measurement results are compared with a numerical simulation by a finite element analysis in explicit mode using Abaqus© code. Section 2 deals with laser-induced shock waves and section 3 introduces a laser-Doppler interferometer and the experimental setup. Section 4 shows a comparison between experimental results and the numerical simulation.

2. Laser-induced shock wave

Laser-induced shock wave has been increasingly used for material processing like laser shot peening [7], adhesion test [8], cladding or stamping. A high-energy pulsed laser beam of energy E and pulse duration at half maximum τ is focused on the surface S of the material. If the light power density Φ impinging on the surface is sufficiently high (typically Φ > 0.1 GW/cm²), a tiny layer is sublimated or ablated. The matter, transformed in plasma, expands and pushes in the direction normal to the sample, creating a strong wave, which for a very high laser power, can be a shock wave (Fig. 1a). As this shock wave propagates, it is followed by a release wave (when pressure falls down). Also, when the shock wave encounters a medium of lower acoustic impedance $Z=\rho C$ (with density ρ and sound velocity C), it is reflected as a release wave. This release wave crosses the release wave of the unloading and an important tensile stress occurs. By tuning the shock parameters and the material properties, it is possible to control the intensity and the location of this tensile stress [8].

When the laser energy is deposited on the sample under a confinement layer (glass, water), the plasma expansion is retained and thus, pressure load and maintaining time are increased [9]. The maximum pressure load generated during such a laser-matter interaction for a Nd-YAG laser with a 10 ns pulse duration and 1.06 µm wavelength [10] is given by

$$\mathrm{P(kBar)} = 0.1\sqrt{\frac{\alpha}{\alpha+3}}\sqrt{Z(g.cm^{-2}.s^{-1})}\sqrt{\phi(GW/cm^{2})} \qquad (1)$$

where α is a laser-matter interaction coefficient, Z is the equivalent acoustic impedance $\frac{2}{Z} = \frac{1}{Z_{water}} + \frac{1}{Z_{sample}}$.

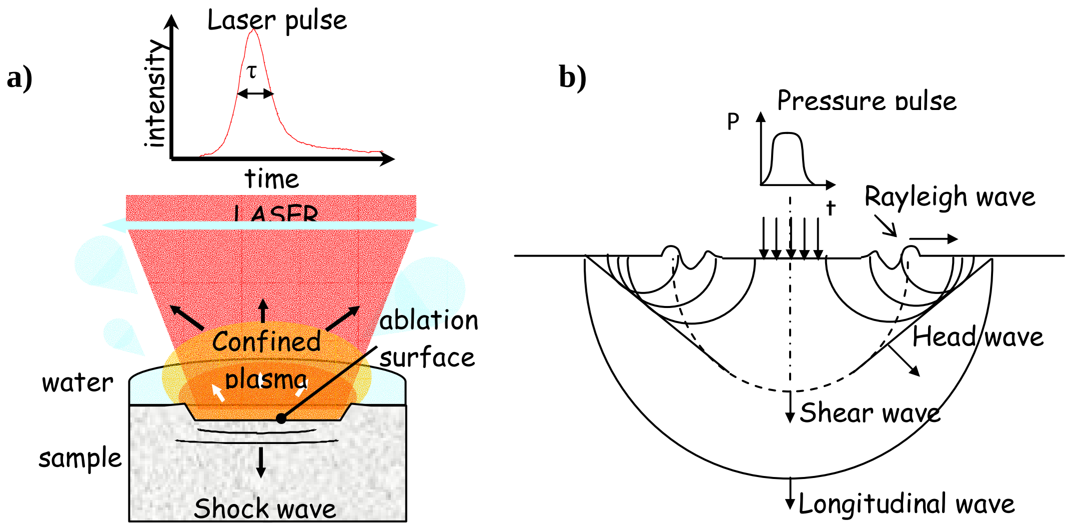

Figure 1. a) Laser-matter interaction in confined regime and b) different type of waves in metals.

In solid materials, there are actually many wave modes generated after an impact (Fig. 1b). When the generated wave is of weak amplitude, a longitudinal wave is propagating forward. This wave is mostly in compression mode and it has the highest intensity and velocity compared with shear and head waves. The shear or transversal wave has a velocity typically of half of the longitudinal wave. The Rayleigh wave is a surface wave and the head wave is an oblique wave between the shear and the longitudinal waves, and is a longitudinal mode consisting of traction and compression (mode I) [11].

3. Shock detection and velocity measurement

In shock experiments, the most accessible shock variable is the material velocity *u* of the opposite surface (free surface) of the impact. One of the most usual method to measure the free surface velocity is the Laser-Doppler Interferometry (LDI). For this work, an etalon based Fabry-Perot LDI has been designed [12]. It is able to measure velocities from 0.5 m/s up to 300 m/s, without contact, at a high repetition rate. The sensing spot for these experiments is about 300 µm of diameter.

The experimental setup is shown in Figure 2a. Shock generation is performed by a 2.5 J Nd-YAG high energy pulsed laser, cadenced at 10 Hz, with a 1.06 µm wavelength and a 10 ns pulse duration. The laser is focused on a 1 cm thick aluminium target, with a spot of 1.3 mm diameter. Shots are performed under water confinement and the laser generation beam is mounted in a X-Y translation stage in order to move the generation beam accurately between two shots. Acquisition of the free surface velocity is synchronized with shock generation and sample displacement. The pressure load generated by the laser ablation was estimated to be about 1.1 GPa.

Series of shots were performed along a line on the sample with a laser beam displacement of 0.5 mm between two shots and the detection fixed (Fig. 2a). For each shot, the free surface velocity as a function of time was recorded. The velocity signals along the path are grouped to form a B-scan image (Fig. 2b), in which colors red and blue are respectively positive and negative velocities. The total distance scanned by the generation laser beam is 20 mm. In the B-scan, the shortest time for which the longitudinal wave breaks out is at the epicentre. The corresponding velocity signal is shown on the left of the B-scan.

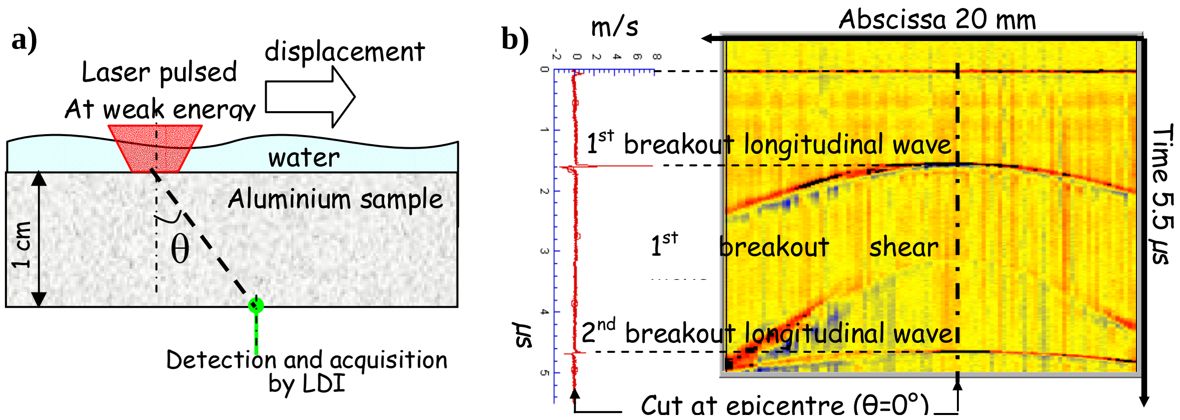

Figure 2. a) Experimental setup and b) B-scan with the velocity signal at epicentre.

4. Numerical simulation

A numerical simulation was performed with the finite element analysis code ABAQUS®. The mesh was structured with square elements in the 2D axisymmetric configuration with semi-infinite elements on the sample side to simulate an infinite plane and to avoid wave rebounds. The Johnson-Cook [13] constitutive law (Eq. 2) was used to represent the elasto-plastic behaviour of the aluminium sample. The set of Johnson-Cook coefficients used are shown in Table I. It was found in preliminary experiments that this equation gives satisfying results.

$$\sigma_{VM} = \left(A + B(\varepsilon_p^{eq})^n\right)\left(1 + C\ln\frac{\dot{\varepsilon}}{\dot{\varepsilon}_0}\right)\left(1 - \left(\frac{T - T_0}{T_{fusion} - T_0}\right)^m\right) \qquad (2)$$

Table 1. Properties of aluminium used for the simulations

	Johnson-Cook coefficients for Al								Shock coefficients		
	A MPa	B MPa	n	C	m	T_{fusion} °K	T_0 °K	P kg/m^3	C_0 m/s	s	Γ (*)
Al	120	300	0.33	0.1	1	916	300	2700	5380	1.339	2

(*) Γ is the Grüneisen coefficient.

Although the color scales are not the same in Figures 3a and 3b, the B-scan obtained by numerical simulation shows the same features as the B-scan obtained by the experiment. From the upper part of the picture, a curved line going down represents the first arrival of the longitudinal wave, noted L_1. Shear wave and head wave are respectively noted S_1 and H_1. Vertical dashed lines are the locations of the free surface velocity signals shown in Figure 4.

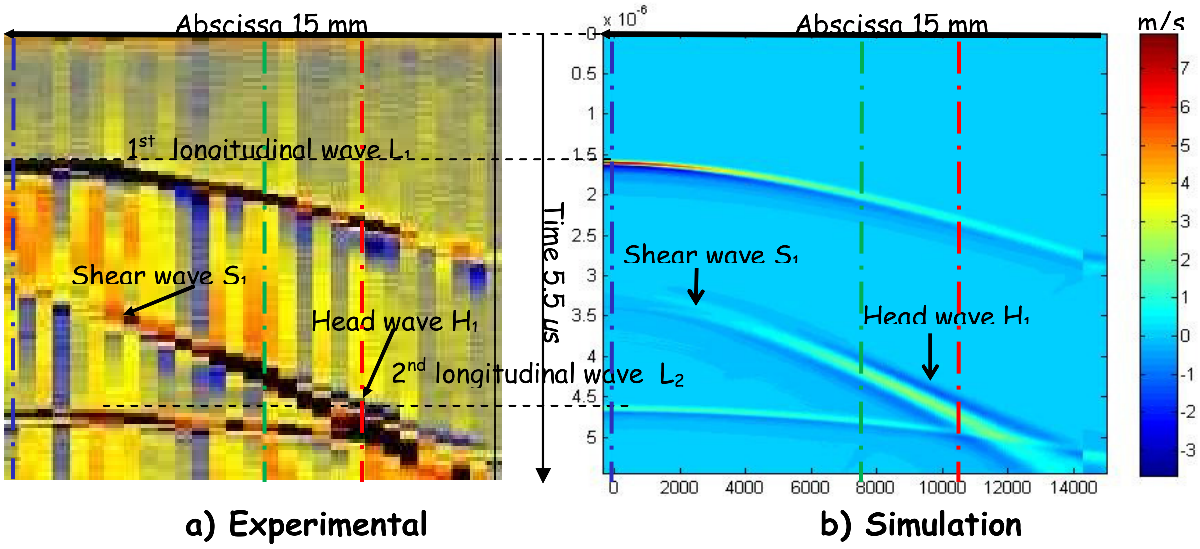

Figure 3. a) Experimental B-scan on an Al sample 1 cm thick and b) B-scan obtained with Abaqus. Vertical dashed lines are locations of velocity signals in Figure 4.

Cuts in the B-scans correspond to θ = 0°, 35° and 45° (θ is defined in Fig. 2a) respectively as blue, green and red lines. At the epicentre (blue line, θ=0°), the signal shows that maximum material velocity of the free surface is under-estimated by numerical simulation. The first arrival occurs at about 1.6 µs for a 1 cm thick aluminium sample. It gives a longitudinal velocity of 6250 m/s, which is very close to the longitudinal velocity for aluminium. In all cases, the free surface velocity has a strong positive spike followed by a weaker negative valley. A positive free surface velocity means a compressive wave and a negative value corresponds to a tensile wave.

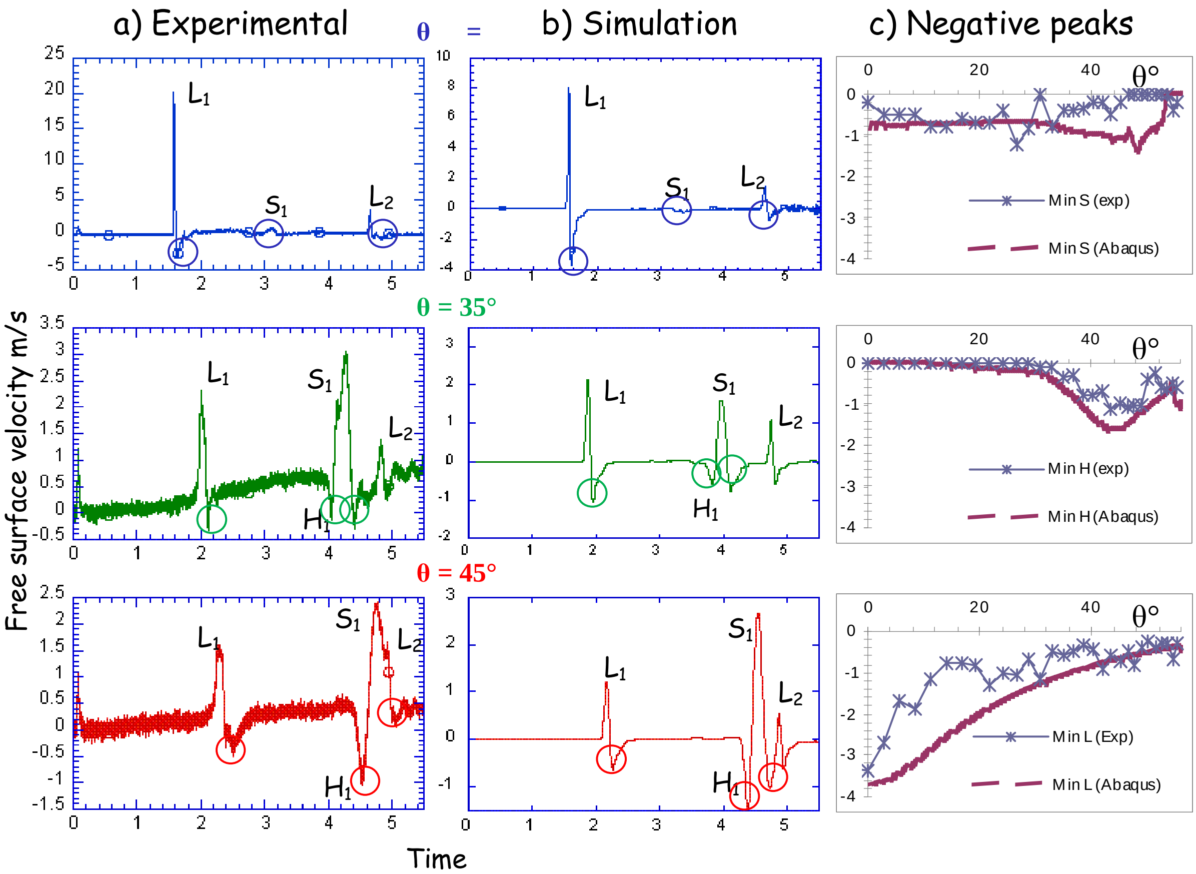

Figure 4. Free surface velocities corresponding to B-scan cuts: a) experiments, and b) simulations. c) Evolution of negative peaks for each wave (S1, H1 and L1 from top to bottom) at an angle θ.

In Figure 4c, the velocities of negative peaks are plotted versus the angle θ. Despite some discrepancies, the evolution of the simulated and experimental velocities are similar. It is then deduced that the highest tensile stress is brought by the L_1 wave on a large angular interval around the epicentre. The tensile stress carried by H_1 wave, that has a maximum around θ=35°, is not as high as the tensile stress of L_1 wave at the epicentre. Also, the tensile stress carried by S_1 wave was found to be marginal.

5. Conclusion

The experimental work and the simulation of waves generated in strong laser ablation show that dynamic tensile stresses can be produced. This tensile stress state can be used to probe adhesive bonding, where weak bonds would break under the test but good bonds would be unaffected by this non-destructive test. It is found that the maximum tensile stress is brought by the longitudinal wave and are due to edge effects. Head waves also create tensile stress but in a lower extent and at a different angle.

Acknowledgement

Authors are grateful to the National Research Council of Canada for its support through the Natural Sciences and Engineering Research Council of Canada. Authors are also grateful to A. Nême and N. Jacques from ENSIETA for their support on Abaqus calculation.

References

1. J.-P. Monchalin, “Laser ultrasonics : from the laboratory to industry”, Keynote presentation at the Review of progress in QNDE, AIP Conference proceedings, eds Thompson and Chimenti, vol 23A, pp. 3-31, 2004.
2. M. Dubois and T. E. Drake, “Super High Quality Laser-ultrasound Signals for Aircraft Component Inspection”, Journal de Physique, 125, pp. 312-320, 2005.
3. J. Yuan and V. Gupta, “Measurement of Interface Strength by the Modified Laser Spallation Technique”, Journal of Applied Physics, 74, pp 2388-2410, 1993.
4. M. Boustie, E. Auroux and J.-P. Romain, “Application of the laser spallation technique to the measurement of the adhesion strength of tungsten carbide coatings on superalloy substrates”, Eur. Phys. J. AP 12, pp. 47-53, 2000.
5. G. Rosa, R. Oltra, M.-H. Nadal, “Laser induced decohesion of coatings: probing by laser ultrasonics” Ultrasonics 40, pp. 765–769, 2002.
6. R. Bossi, K. Housen and W. Shepherd, “Using Shock Loads to Measure Bonded Joint Strength”, Materials Evaluation, 60, pp. 1333-1338, 2002.
7. P. Peyre, R. Fabbro, P. Merrien, H.P. Lieurade, “Laser shock processing of aluminium alloys. Application to high cycle fatigue behaviour”, Materials Science and Engineering A210, pp. 102-113, 1996.
8. C Bolis, L Berthe, M Boustie, M Arrigoni, S Barradas and M Jeandin “Physical approach to adhesion testing using laser-driven shock waves”, J. Phys. D: Appl. Phys. 40, pp. 3155–3163, 2007.
9. R. Fabbro, J. Fournier, P. Ballard, D. Devaux, and J. Virmont, J. Appl. Phys. 68, p. 775, 1990.
10. L. Berthe, R. Fabbro, P. Peyre, L. Tollier and E. Bartnicki “Shock waves from a water-confined laser-generated plasma”, J. Appl. Phys. 82, 1999.
11. J.-P. Monchalin, R. Héon, J. Bussière and B. Farahbakhsh, Nondestructive characterization of materials II, Plenum Press, pp. 717-723, 1987.
12. M. Arrigoni, S. E. Kruger, A. Blouin, D. Levesque, M. Lord, J.-P. Monchalin, “The use of Laser-Doppler Interferometry based on a Fabry-Perot Etalon for Shock Adhesion Test applied to adhesively bonded Materials”, this conference Laser Ultrasonics 2008, Montreal, 2008.
13. G.R. Johnson and W.H. Cook, “A Constitutive Model and Data for Metals Subjected to Large Strains, High Rates and High Temperatures”, Proc. of the 7th International Symposium on Ballistics, The Netherlands, pp.541-547, 1983.